

Synchronization of Pulse-Coupled Oscillators for IEEE 802.15.4 Multi-hop Wireless Sensor Networks

Yan Zong, Xuewu Dai, Zhiwei Gao, Krishna Busawon, Richard Binns, Ian Elliott

Department of Mathematics, Physics and Electrical Engineering

Northumbria University

Newcastle upon Tyne, United Kingdom

{yan.zong, xuewu.dai, zhiwei.gao, krishna.busawon, richard.binns, i.d.elliott}@northumbria.ac.uk

Abstract—As a key enabling technology in mission-critical Wireless Sensor Networks (WSNs), time synchronization provides a common timescale for distributed sensor nodes in many wireless applications, such as coordinated control and underwater navigation and tactical surveillance. Inspired by the behaviour of fireflies, along with mathematical model, Pulse-Coupled Oscillators (PCO), has been proposed to enable synchronization in complex networks, where all the PCO's firing signal *Pulses* are broadcasted simultaneously when synchronization is achieved. The requirement of zero-drift clock oscillators, fully-connected network and concurrent transmission of *Pulses* are, in reality, impossible to achieve. To avoid transmission collision and enable the PCO extension in the multi-hop WSNs, the *desynchronization* mechanism is adopted to enable the *Pulse* packets to be transmitted to the wireless channel in a uniformly distributed fashion. Due to the contention-free period's feature of low-latency, thereby avoiding the need to wait for a random and potentially long period until the channel is available, the PCO's *Pulse* packets are transmitted in the contention-free period of IEEE 802.15.4-2015 superframe. Thus, a novel state-space model for *desynchronization*-based pulse-coupled non-identical oscillators is proposed to model a realistic drifting clock oscillator. Moreover, the timestamped *Pulse* packets are transmitted to determine the offset of connected sensor nodes, and an attenuated clock correction scheme is adopted to correct the local drifting clocks by using measured offset and skew. The intensive simulations of the three-hop three-cluster wireless network and the seven-hop linear network have been carried out to evaluate performance of timestamped PCO with *desynchronization* method.

Index Terms—time synchronization, pulse-coupled oscillators, *desynchronization*, IEEE 802.15.4, multi-hop wireless sensor networks

I. INTRODUCTION

In many mission-critical applications of Wireless Sensor Networks (WSNs), a network of distributed sensors needs to work cooperatively to monitor events or objects, and requires high precision common sense of timing among sensor nodes. Time Synchronization (TS) is a key enabling technology in such time-sensitive wireless sensor networks. Typical examples are coordinated motion control, collaborative condition monitoring, intruder detection and time-of-flight location.

However, due to the manufacturing tolerance of low-cost embedded systems, the sensor node local clock, which commonly takes the form of a crystal oscillator, is subject to variation in phase and frequency. In addition to manufacturing tolerance, local clock frequency may also drift due to envi-

ronmental conditions, such as temperature and power supply voltage. The goal of time synchronization is to keep the offset and drift of these non-identical sensor node clocks as close to zero as possible. Finally, all the clocks in a sensor network have the same timescale once the synchronization is achieved.

Mathematically speaking, the purpose of TS is to keep the sensor node clocks' offset and drift as small as possible. In the communication engineering community, many different TS protocols have been proposed for wireless sensor networks, examples being Precision Time Protocol (PTP) [11] and Reference Broadcast Synchronization (RBS) [5]. These protocols are based on periodical timestamped packet exchange among paired and connected nodes to acquire the time difference of two clocks. Once the time difference is obtained, a sensor node corrects its clock's offset and drift accordingly, in order to approach the *reference time*. It is well known that, in the multi-hop large-scale wireless sensor networks, since the synchronization error in each hop is accumulated, the accuracy of such TS protocols is diminished by the increase in hop distance.

Owing to its foundation and significance, synchronization is also of interest to the mathematics and physics communities, where it is applied to networked oscillators consisting of a set of oscillators whose phases are pair-wise coupled. The so-called Pulse-Coupled Oscillators (PCO), being a typical model of networked oscillators, is inspired by synchronous flashing of fireflies observed in certain parts of southeast Asia. The pulse-coupling of PCO is episodic and pulse-like [14].

A. Related Work

In the classical PCO, an oscillator works in either free-running mode or interactive mode. In the free-running mode, the oscillator behaves as an uncoupled oscillator. In this mode, the clock state, which is denoted by P , rises toward a threshold value. When the clock state reaches the threshold, the oscillator fires, resulting in a *Pulse* being generated whilst P is reset, after which the cycle repeats.

Packet-exchange time synchronization in WSNs can be modelled as pulse-coupled oscillators, where the periodical packet transmission is equivalent to *Pulse* firing. From the viewpoint of PCO, the clocks in the wireless sensor nodes are equivalent to oscillators in PCO. It is common scenario that the clock signal in an embedded system is implemented

by a *counter* driven by a crystal oscillator. The *counter* is reset when its value reaches a predefined threshold. This indeed is similar to the firing-resetting procedure of PCO, where the oscillator fires and its state is reset to zero periodically [19]. Therefore, the term *oscillator* will be used when describing the PCO model, the term (*wireless sensor*) *node* is adopted when describing the model implemented in WSNs, and the wireless *Pulse* packet is adopted to describe the *Pulse* of classical PCO model.

Due to its inherent scalability and simplicity which are beneficial when applied to the large-scale distributed wireless networks with low-energy cost, PCO has also attracted a lot of attention over the years. Nevertheless, two classical PCO's assumptions, (i) they have identical internal dynamics of oscillators (i.e., the frequencies of all oscillators are same) and (ii) they employ an all-to-all coupling strategy (i.e., fully-connected network topology), restrict the application to the realistic large-scale WSNs. This paper focuses on the problems of mismatched oscillators (i.e., drifting clock) and partially-connected network topology (i.e., multi-hop large-scale wireless sensor networks).

In the interactive mode of classical PCO, the clock state evolves as mentioned in the free-running mode. In addition, the clock state P is pulled up by a specific constant coupling strength (i.e., excitatory coupling), upon the reception of a *Pulse* from another oscillator. All the oscillators of a network will broadcast *Pulses* simultaneously when the synchronization is achieved in the network.

Typically, WSNs consisting of a large number of wireless nodes will involve a large number of *Pulse* packets being transmitted to the single wireless channel at the same time, when the synchronization of the sensor network is achieved. As a consequence, the *Pulse* packets from all the transmitting sensor nodes will interfere with each other (known as transmission collision) and no packets can be successfully received. To address this issue, [2] proposed the technique of *desynchronization* (DESYNC), this being the logical opposite of synchronization, in order to ensure the *Pulse* packets be transmitted in a uniformly distributed fashion, thereby minimising the possibility of collision.

[2] proposed and implemented the *desynchronization* in the single-hop wireless sensor networks. When DESYNC was achieved in the wireless networks, N sensor nodes were able to transmit the *Pulse* packets with the specified interval space T/N during one time synchronization cycle T . In the existing literatures [1], [2], [3], they provided no solution for separating the control traffic (i.e., the *Pulse* packets) from the data traffic transmitted on the same wireless channel. This means that, only time synchronization was taken into account. In [7], a proposal was made for a scheduling protocol that allows natural separation of the control traffic from the data traffic transmitted on the same wireless channel. Moreover, it also extended the DESYNC to the clustered wireless sensor networks (i.e., multi-hop wireless sensor networks). However, the aforementioned approaches still lack the compatibility between the DESYNC and the superframe of beacon-enabled

operation, as specified in IEEE 802.15.4-2015. Moreover, all the pulse-coupled oscillators in literatures [1], [2], [3], [7], [16] were identical internal dynamics and all oscillators' frequencies were same. This is not true when it comes to any real-world environments, and the gap exists between the PCO mathematic model and the oscillators in real world, the realistic drifting pulse-coupled oscillators model is also needed.

B. Desynchronization-based Pulse-Coupled Oscillators

In the beacon-enabled operation of IEEE 802.15.4-2015 [12], a superframe, bounded by two neighboring beacons, has three periods, namely - Contention Access Period (CAP), Contention-Free Period (CFP) and Inactive Period. During the CFP, a time slot is guaranteed for a specific node and Time-Division Multiple Access (TDMA) is used for channel access [6].

In PCO model, when the clock state reaches the threshold, a *Pulse* packet is generated, transmitted and received simultaneously. This means that the delay from the time that a *Pulse* packet is generated to the point at which it is received should be as small as possible. Benefiting from the feature of low-latency in CFP, namely, avoiding waiting for a random and potentially long period of time until the channel is available, the *Pulse* packets of pulse-coupled oscillators can be transmitted in the CFP of superframe.

To derive an accurate model for a realistically drifting *desynchronization*-based PCO clock and enable the compatibility between the pulse-coupled oscillators and IEEE 802.15.4-2015 superframe, the behaviour of the clock is modelled by using the state-space approach. This approach is also considered in several works (e.g., [8], [10] and [19]), and has the advantage that specific features of clock behaviour can be described.

Moreover, the *Pulse* packets, containing timestamps generated by local clocks, are transmitted to estimate the offset and drift of local drifting clocks, and an improved clock correction mechanism, known as the attenuated correction scheme, is adopted to correct the local drifting clocks.

C. Contribution and Paper Organization

In this paper, a novel state-space model for *desynchronization*-based pulse-coupled drifting oscillators is proposed, and the proposed PCO clock model enables the PCO extension of large-scale wireless sensor networks while achieving compatibility with existing IEEE 802.15.4-2015. Additionally, the timestamped *Pulse* packets are transmitted to estimate the offset of connected sensor nodes, and an attenuated clock correction scheme is adopted to correct the local drifting clocks. Furthermore, two scenarios of network topologies, namely, the three-hop three-cluster wireless network and the seven-hop linear wireless network are simulated to evaluate the performance of the proposed *desynchronization*-based PCO synchronization.

The rest of this paper is as follows: the proposed *desynchronization*-based PCO clock model is derived in Section

2. Next, in Section 3, the timestamp which is generated on local clock time based on the reception of received *Pulse* is introduced, and the clock offset and skew measurements and correction algorithms are also presented. Simulation results are given in Section 4. Finally, conclusions are presented in Section 5.

II. DISCRETE MODEL OF A DESYNCHRONIZATION-BASED NON-IDENTICAL PULSE-COUPLED OSCILLATOR CLOCK

One of the considered network topologies in this paper, the cluster-tree network, is exemplified in Fig. 1. The network is identified by the *root node*, which is unique and is equipped with a Global Positioning System (GPS) clock to provide *reference clock* to all sensor nodes. Each *internal node* (also known as *branch node*) is any node of a tree that has child nodes. And the *leaf node* is the node without any child nodes. The cluster-tree is formed by several parent-to-child associations between *branch* and *leaf nodes* up to a certain level. In Fig. 1, for instance, B1 is a parent *branch node* of B4 and a child *branch node* of the network *root node*. Throughout this paper, the *reference clock* is referred to as the master clock, and the *root node* and *branch* (and *leaf*) *node* are called master node and sensor node respectively.

It is important to remark that, the PCO model of time synchronization in such a practical wireless sensor network differs from the classical PCO in two aspects: (i) a master oscillator presents and works as a pacemaker, (ii) the sensor node oscillators are non-identical. The master node clock can be regarded as a perfect oscillator running at a precise nominal frequency with zero initial phase. The sensor node clocks can be regarded as drifting non-identical oscillators with unequal nominal frequencies and different initial phases [19].

It is well known that in the embedded systems, the discrete clock consists of (i) a crystal oscillator running at a specified frequency; (ii) a *counter* that counts the number of clock ticks generated by the oscillator. Assume a crystal oscillator runs at its nominal frequency f_0 and the discrete clock is updated periodically at an interval $\tau_0 = 1/f_0$. Let $t[n]$ denote the actual time at the n -th clock update event, $t[n]$ is also known as the *reference time*. For a perfect clock, such as the GPS clock at *root node*, $t[n] = n\tau_0$.

In the free-running mode of PCO, the clock state which is represented by a state variable P increases linearly from zero to threshold value defined by φ . Once P reaches the threshold φ , P is reset to 0, followed immediately by a *Pulse* that is fired and broadcasted to other oscillators for synchronization purpose. Similarly, in WSNs, the threshold of a *counter* can be set to the same value of φ in order to achieve the same time synchronization cycle (i.e., $\varphi = T$). Let $N_i[n]$ denote the total number of the i -th PCO fires at present n -th clock update. If the PCO clock fires at the n -th clock update event, $N_i[n] = N_i[n-1] + 1$, and the dynamic of $N_i[n]$ can be represented as

$$N_i[n] = \begin{cases} N_i[n-1], & \text{if } P_i[n] < \varphi_i \\ N_i[n-1] + 1, & \text{if } P_i[n] \geq \varphi_i \end{cases} \quad (1)$$

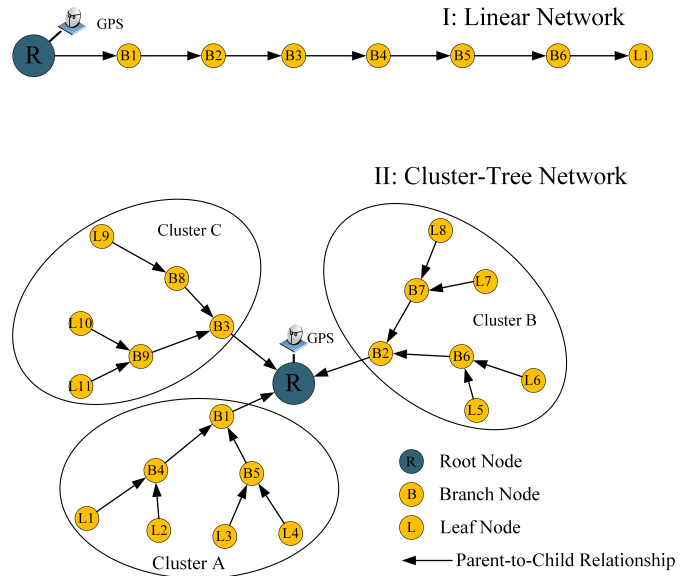


Fig. 1. Network topologies (I: seven-hop linear wireless network, II: three-hop three-cluster wireless network).

It is notable that in the embedded systems, the physical waveform (i.e., *Pulse*) of classical PCO cannot be generated and broadcasted, however, the packet named with *SYNC* can be adopted to mimic the PCO *Pulse*. Therefore, the *Pulse* is referred to as *SYNC* packet thereafter in this paper.

In the interactive mode, the state variable evolves as mentioned above, in addition, the clock state is corrected when receiving the *SYNC* packets from other sensor nodes. Furthermore, a *SYNC* packet is generated and transmitted immediately if the corrected state variable exceeds the threshold. All the sensor nodes will transmit *SYNC*s simultaneously when synchronization of the network is achieved.

It is often the case, that in the large-scale wireless sensor networks consisting of huge amounts of nodes, *SYNC* packets from synchronized sensor nodes interfere with each other and no packets can be received successfully. To address this issue, the concept of *desynchronization* is adopted, and all the *SYNC* packets generated by sensor nodes are therefore transmitted in a uniformly distributed fashion and in the CFP of IEEE 802.15.4-2015 beacon-enabled operation superframe.

However, in the CFP of beacon-enabled superframe, the number of Guaranteed Time Slots (GTSS) can be allocated up to seven at the same time [12]. Theoretically, only 7 sensor nodes in same cluster are allowed to simultaneously transmit the packets to the wireless channel. If the total number of sensor nodes in the same cluster is greater than 7, the technique, such as the graph colouring [13] or space-division multiplexing, can be adopted to increase the capability of proposed superframe.

The proposed superframe in Fig. 2, bounded by neighbouring *SYNC* packets by the *root node*, consists of three types of periods, namely - Scheduled Offset (SO), *DESYNC* and

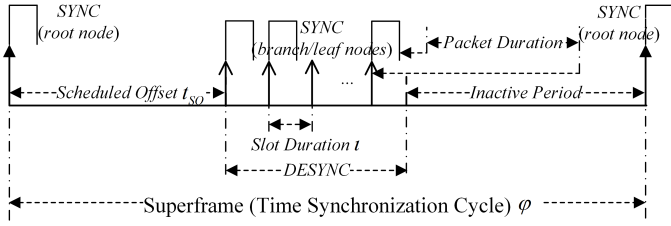


Fig. 2. The Proposed Superframe.

Inactive Period. The SO, corresponding to the CAP, is used to transmit the data by Carrier-Sense Multiple Access with Collision Avoidance (CSMA-CA) mechanism. The *DESYNC*, which corresponds to the CFP, enables sensor nodes (including the *branch* and *leaf nodes*) to transmit the *SYNC* packets to achieve the *desynchronization* by using the TDMA mechanism. In addition, the Inactive Period is used to let the sensor nodes sleep, in order to reduce the power consumption.

Taking the periodical resetting behavior of PCO and implementation of *desynchronization* into account, at the n -th clock update event, the i -th drifting PCO clock's state $P_i[n]$ can be modelled as

$$P_i[n] = t[n] + \frac{\sum_{n=0}^{n-1} \alpha_i[n] \tau_0}{f_0} + \phi_i[n] - \sum_{n=1}^{N_i[n]} \varphi_i[n] - t_{d_i} \quad (2)$$

where $\alpha_i[n]$ denotes the frequency deviation of the drifting oscillator at $t[n]$, $\phi_i[n]$ is the instant phase noise (which can be modelled as a random process), and $t_{d_i} = t_{SO} + (i-1) \times \iota$ represents the i -th PCO clock's *desynchronization* offset. Moreover, t_{SO} is the duration of SO, and ι means the *slot duration* (representing the time between neighboring *SYNC*s from *branch* or *leaf nodes*). The *packet duration* is the time that a complete *SYNC* packet requires for transmission over the wireless channel.

Clock offset is the difference between the i -th drifting PCO clock $P_i[n]$ and the *reference clock* $t[n]$. To obtain a more succinct PCO clock model, it can be seen from (2) that the clock offset $\theta_i[n]$ of the i -th sensor node in the embedded systems is the accumulated phase deviation caused by drifting frequency $\frac{\sum_{n=0}^{n-1} \alpha_i[n] \tau_0}{f_0}$, phase noise $\phi_i[n]$ minus the sum of threshold $\sum_{n=1}^{N_i[n]} \varphi_i[n]$. That is

$$\theta_i[n] = \frac{\sum_{n=0}^{n-1} \alpha_i[n] \tau_0}{f_0} + \phi_i[n] - \sum_{n=1}^{N_i[n]} \varphi_i[n] \quad (3)$$

In the discretized clock model, the skew $\gamma_i[n] = \frac{\alpha_i[n]}{\tau_0}$, a dimensionless quantity, can be adopted to denote the deviation of frequency from the nominal frequency f_0 for one clock update interval of $[t[n], t[n+1]]$. Therefore, by introducing $\omega_{\theta_i}[n] = \phi_i[n+1] - \phi_i[n]$, the offset of the $(n+1)$ -th event is

$$\theta_i[n+1] = \begin{cases} \theta_i[n] + \gamma_i[n] \times \tau_0 + \omega_{\theta_i}[n], & \text{if } P_i < \varphi_i \\ \theta_i[n] + \gamma_i[n] \times \tau_0 + \omega_{\theta_i}[n] - \varphi_i, & \text{if } P_i \geq \varphi_i \end{cases} \quad (4)$$

[9] introduces the first-order auto-regressive model, by considering the phase noise of oscillator and clock skew with a certain randomness that is not completely independent for each sample. According to the assumption that the skew $\gamma_i[n]$ is of slow change as well, the skew of the $(n+1)$ -th event, described as a time-varying process in an auto-regressive manner with a small perturbation, is defined as

$$\gamma_i[n+1] = p \times \gamma_i[n] + \omega_{\gamma_i}[n] \quad (5)$$

where p , denoting the parameter of first-order auto-regressive model, is a positive number less than but close to 1, and ω_{γ_i} indicates the model noise with zero mean. In addition, both offset noise ω_{θ_i} and skew noise ω_{γ_i} , two uncorrelated random process, are subjected to zero-mean gaussian distribution with standard deviation σ_{θ_i} and σ_{γ_i} respectively [19].

It is worth noting that the clock model of (2),(4),(5) can represent both a perfect, non-drifting, clock and a drifting PCO clock. If both clock offset and skew are zero (i.e., $\theta_i[k] = 0$, $\gamma_i[k] = 0$, $\omega_{\theta_i}[k] = 0$ and $\omega_{\gamma_i}[k] = 0$), the clock is a perfect clock without frequency drifting. Otherwise, the (2),(4),(5) are to generate the drifting PCO clock time information.

III. LOCAL TIMESTAMP AND CLOCK CORRECTION MECHANISM

The proposed clock measurement algorithm provides the means for estimating the offset and drift of a local drifting clock through the reception of the *SYNC* packet containing a timestamp generated by the local clock. Once a timestamp of packet is obtained, the offset between two nodes can be determined, and an improved clock correction mechanism, known as the attenuated correction method, is adopted to correct the clock offset and skew of a drifting PCO clock.

A. Local Timestamp

To be more specific, at the k -th time synchronization cycle, both sensor node i and j fire and transmit the *SYNC* packets at their allocated slot. Upon the reception of the *SYNC* from node j , node i reads its local clock, generates a timestamp $\bar{P}_{ij}[k]$ and associates it to the received *SYNC* packet.

There are two ways to generate a timestamp, namely, *hardware timestamping* and *software timestamping*. *Hardware timestamping* requires additional carefully designed hardware, it is precise, but is too expensive to be implemented in most low-cost wireless sensor nodes. Instead, *software timestamping* is widely used in WSNs, where the timestamp is generated by software code via reading a *counter* driven by a crystal oscillator, either in an interrupt or a polling scheme. *Software timestamping* does not require additional hardware, but delays and uncertainties are introduced for the micro-processor to execute the code of clock reading. Furthermore,

if the *software timestamping* is implemented at higher layer (e.g., the *application layer*), the packet processing time for a packet to pass from *physical layer* to upper layer is much longer and with more uncertainties, such as scheduling delay of operation system, queueing, media access delay, and so on. The measurement offset and skew are therefore affected by the local clock timestamp uncertainty ΔP , which is denoted by random variables with finite standard deviation σ_η whose value can be varied to consider different timestamping performances [8]. And the timestamp $\bar{P}_{ij}[k]$ of the i -th sensor node at the k -th time synchronization cycle is

$$\bar{P}_{ij}[k] = P_i[k] + \nu_{\theta_{ij}}[k] \quad (6)$$

where $\nu_{\theta_{ij}}[k] = \Delta P_{ij}[k]$ is the measurement offset uncertainty with standard deviation $\sigma_{\eta_{ij}}$. By introducing the timestamp uncertainties, the variations of transmission, propagation and processing delays are taken into account, hence making the model more realistic. It is worth noting that timestamp uncertainty is a non-zero noise; however, in the future, it can be estimated by adopting the statistics solution, and the estimated value will be used to compensate the offset measurement.

B. Clock offset Measurement and Correction Mechanisms

Once a timestamp of packet is obtained, the offset between two nodes can be determined. Let $\bar{\theta}_{ij}[k]$ denote the offset measurement of node i based on the reception of a *SYNC*, which contains the local timestamp $\bar{P}_{ij}[k]$, from the j -th node at the k -th synchronization cycle, the offset measurement is

$$\bar{\theta}_{ij}[k] = \begin{cases} \bar{P}_{ij}[k] - \kappa - (t_{d_j} - t_{d_i}) & \text{if } \bar{\theta}_{ij}[k] < \frac{\varphi_i[k]}{2} \\ \bar{P}_{ij}[k] - \kappa - \varphi_i[k] - (t_{d_j} - t_{d_i}) & \text{if } \bar{\theta}_{ij}[k] \geq \frac{\varphi_i[k]}{2} \end{cases} \quad (7)$$

where κ is the transmission delay.

Since the clock offset after the correction is unknown, however it is close to zero, assumption is given that the drifting clock is corrected in the last synchronization cycle (i.e., $\bar{\theta}_{ij}[k-1] = 0$). The skew is also assumed to be constant in one time synchronization cycle φ , therefore, the clock skew of the i -th node can be estimated as

$$\bar{\gamma}_{ij}[k] = \frac{\bar{\theta}_{ij}[k]}{\varphi_i} \quad (8)$$

where $\bar{\gamma}_{ij}[k]$ can be regarded as the measurement of clock skew $\gamma_i[k]$.

In real WSNs, the offset and skew measurements suffer from various timestamp noises and uncertainties. As a result, the over-correction may occur and the time synchronization performance degrades. Instead of using the whole measured offset and skew to correct the clock directly, by adopting the attenuated clock correction scheme, the drifting clock is corrected by a relatively attenuated amount of the offset and skew measurements for better synchronization performance. Over-correction can also be avoided at the cost of taking a relatively longer time to synchronize the sensor node drifting

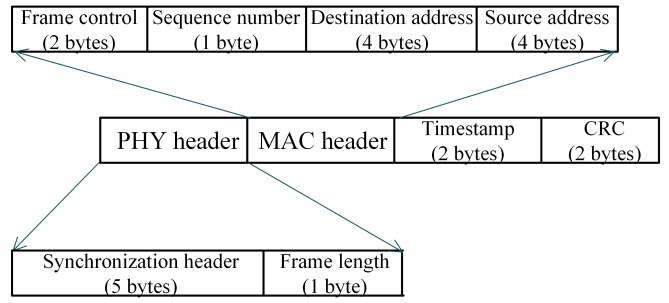


Fig. 3. The format of a *SYNC* packet.

clocks to *reference clock* [10]. The attenuated correction scheme only adjusts the offset and skew by a portion of the offset and skew measurements, respectively

$$\begin{cases} \theta_i[k]^+ = \theta_i[k]^- - \alpha \bar{\theta}_i[k] \\ \gamma_i[k]^+ = \gamma_i[k]^- - \beta \bar{\gamma}_i[k] \end{cases} \quad (9)$$

where $\theta_i[k]^+ / \theta_i[k]^-$ is the clock offset after/before the local drifting clock is corrected at the k -th time synchronization cycle. Similarly, $\gamma_i[k]^+ / \gamma_i[k]^-$ is the PCO clock skew after/before the local clock is corrected. α and β are the attenuation coefficients taking values among $(0, 1)$.

IV. SIMULATIONS AND RESULTS

In order to evaluate the proposed synchronization method of timestamped PCO with *desynchronization*, intensive simulations have been carried out on a realistic time synchronization simulator (TS2) developed in [18] on the discrete event simulation platform OMNeT++ [15]. Two scenarios of network topologies, namely, the three-hop three-cluster network and the seven-hop linear network as shown in Fig. 1, are simulated. The drifting clock is taken from [8] and

TABLE I
SIMULATION CONFIGURATIONS

Symbol	Value
Initial offset θ_0	[10ms, 20ms, ..., 190ms, 200ms]
Initial drift γ_0	[0PPM, 5PPM, ..., 90PPM, 95PPM]
Clock update frequency f_0	32.768kHz
Clock state threshold φ	1s
Scheduled offset t_{SO}	500ms
Slot duration ι	[1ms, 10ms]
Packet duration	0.672ms
<i>SYNC</i> packet length	21bytes
Transmission delay κ	0.48ms
(α, β)	(0.6, 0.08)

its offset noise is of zero mean and standard deviation $\omega_\theta = 10^{-7}$, skew noise is of zero mean and standard deviation $\omega_\gamma = 10^{-9}$. The clock update frequency is 32.768kHz to replicate the Real-Time Clock crystal oscillator at SAM R21 [17]. The duration of one time synchronization cycle is 1s, thus the threshold of PCO clock state is configured to 1s. The format of *SYNC* packet is shown in Fig. 3, and the length of packet is 21 bytes according to the ZigBee standards [4],

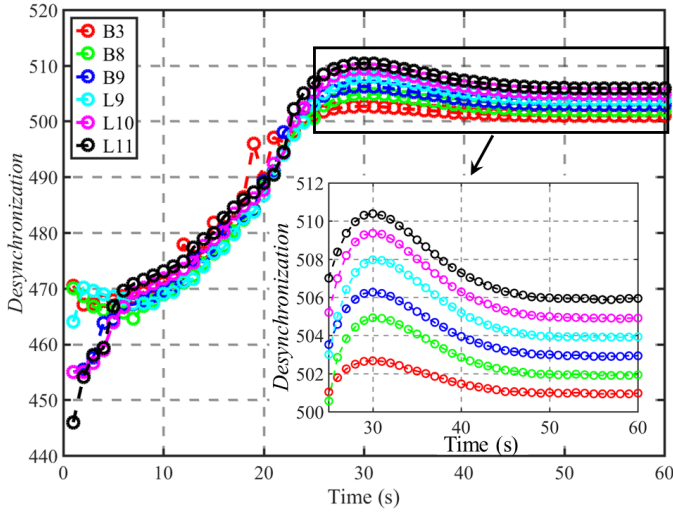


Fig. 4. The proposed *DESYNC* Period in wireless network Cluster C ($\iota = 1ms$).

[6]. Moreover, the timestamp uncertainty is modelled by a random process with standard deviation of 10^{-8} to simulate the *hardware timestamping* [8]. The simulation configurations of the clocks and wireless networks are summarized in Table. 1.

Fig. 4 indicates the *desynchronization* in the Cluster C of a wireless network consisting of 6 sensor nodes. It is clear that after several rounds of time synchronization, six sensor nodes, including *branch* and *leaf nodes*, transmit the *SYNC* packets during the *DESYNC* period which is after the Schedule Offset of $t_{SO} = 500ms$. Furthermore, the *SYNC* packets are transmitted with the specified interval space (i.e., *slot duration* of $\iota = 1ms$). Thus, by implementing the *DESYNC* in IEEE

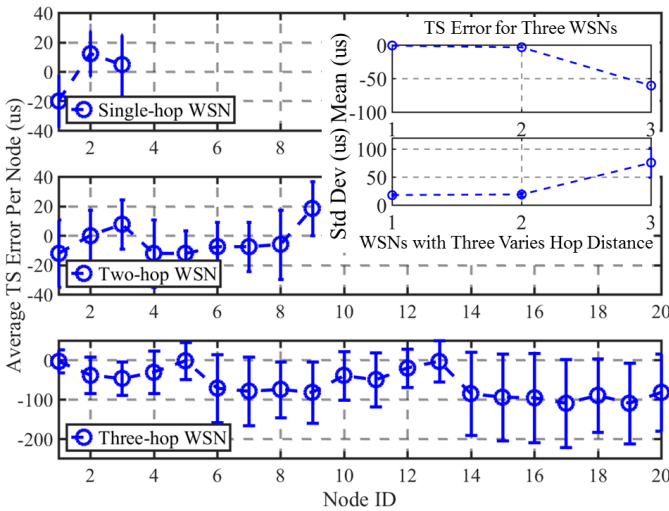


Fig. 5. Average time synchronization error in three WSNs (Single-hop WSN: $\iota = 1ms$, Two-hop WSN: $\iota = 1ms$, Three-hop WSN: $\iota = 10ms$).¹

¹1 \rightarrow B1 (the node with ID '1' is B1 in Fig.1), 2 \rightarrow B2, ..., 9 \rightarrow B9, 10 \rightarrow L1, 11 \rightarrow L2, ..., 20 \rightarrow L11.

802.15.4-2015 superframe, the *desynchronization*-based PCO works correctly. In addition, the simulation of [18] showed that the achieved synchronization in classical non-identical PCO clocks lose gradually. However, by using the attenuated clock correction scheme, the *desynchronization*-based PCO clocks are able to maintain the synchronization since both clock offset and skew of drifting clocks are corrected.

Fig. 5 demonstrates the performance of *desynchronization*-based PCO time synchronization in the three wireless network topologies of Fig. 1, namely, single-hop, two-hop and three-hop WSNs. The circle is the mean of synchronization error with respect to the *reference clock* of *root node*, and the up/low bar represents mean value plus/minus its corresponding standard deviation, representing the variation of the synchronization error for each sensor node clock. The two-hop wireless network can achieve the time synchronization with the precision of $40us$. While in the three-hop network, the accuracy of time synchronization reduces to $250us$ and the synchronization accuracy of sensor nodes with the hop distance of 2 also reduces to $200us$. Since bi-directed coupling (where two connected sensor nodes are able to receive *SYNCs* from each other and correct their own clocks from the received *SYNCs*) is adopted, and all the sensor nodes are equipped with the drifting clocks, both *reference clock* of *root node* and child node drifting clocks have effect on the parent node drifting clock. Therefore, in the multi-hop large-scale wireless sensor network, with the increase of hop distance, WSNs synchronization performance (i.e., average time synchronization error and standard deviation of synchronization error) degrades significantly.

Fig. 6 shows that the performance of two kinds of coupling mechanisms, namely, bi-directed coupling and directed coupling (where only child nodes receive and process the *SYNCs* from its parent node), in the seven-hop linear wireless network. Simulation results show that the mean of synchronization error increases linearly in two kinds of coupling

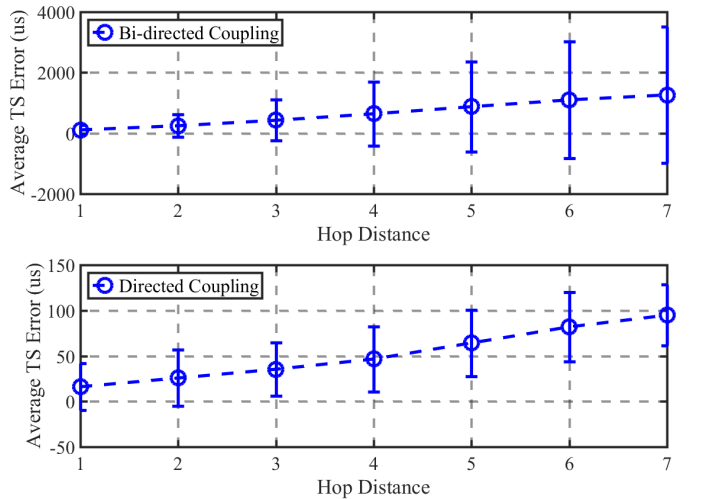


Fig. 6. Average time synchronization error in the seven-hop linear WSN with bi-directed and directed coupling mechanisms ($\iota = 10ms$).

mechanisms. Since directed coupling is adopted, only the *reference clock* of *root node* or parent node clocks have effect on the child node drifting clocks, the synchronization precision of $150\mu s$ can be achieved in seven-hop wireless sensor networks by using directed coupling mechanism. However in the same network topology with the bi-directed coupling mechanism, the standard deviation of synchronization error increases linearly with the increase of hop distance, and the precision of synchronization only is $4000\mu s = 4ms$.

In [16], the synchronization with precision of $100\mu s$ was achieved under MATLAB simulation of the identical oscillators, no propagation delay and transmission delay. Even though [7] achieved the time synchronization with accuracy of fractions of microseconds, the identical oscillators were used and simulated. In the existing work [7], [16], the identical oscillators with zero phase noise and skew noise were simulated. This is not true when it comes to any real-world environments, as all the clocks in the real embedded systems are non-identical and drifting. Moreover, the propagation delay and transmission delay always present. Therefore, the proposed synchronization method of timestamped PCO with *desynchronization* can achieve the better time synchronization with accuracy of $150\mu s$ by using directed coupling mechanism in the seven-hop linear network consisting of non-identical and drifting clocks.

CONCLUSION

In this paper, a novel *desynchronization*-based pulse-coupled non-identical oscillators model is proposed to describe a realistic drifting clock oscillator. The proposed PCO clock model enables the extension of large-scale wireless sensor network and the compatibility of existing IEEE 802.15.4-2015. Moreover, the *Pulse* packets containing the local timestamps are transmitted to measure the offset and skew of connected sensor nodes, and an attenuated clock correction scheme is adopted to correct the local drifting clocks. Additionally, it is shown that the three-hop cluster-tree wireless sensor network consisting of 20 sensor nodes can achieve the synchronization with the precision of $250\mu s$ by using bi-directed coupling mechanism. Similarly, it is demonstrated that the seven-hop linear wireless sensor network obtains the synchronization with the precision of $150\mu s$ when the directed coupling mechanism is adopted. As the basis of future research work, the *desynchronization*-based pulse-coupled oscillators model will be implemented in a realistic hardware testbed, in order to fully evaluate its performance in a real-world context.

ACKNOWLEDGMENT

Yan Zong gratefully acknowledges financial support from the University of Northumbria at Newcastle *via* a postgraduate research studentship.

REFERENCES

[1] D. Buranapanichkit, N. Deligiannis, Y. Andreopoulos., Convergence of Desynchronization Primitives in Wireless Sensor Networks: A Stochastic Modeling Approach, *IEEE Transactions on Signal Processing*, vol. 63, issue 1, pp. 211-233, Jan 2015.

[2] J. Degeys, I. Rose, A. Patel, R. Nagpal., DESYNC: Self-Organizing Desynchronization and TDMA on Wireless Sensor Networks, in *International Conference on Self-Adaptive and Self-Organizing Systems*, Cambridge, USA, 2007, pp.11-20.

[3] J. Degeys and R. Nagpal., Towards Desynchronization of Multi-hop Topologies, in *International Conference on Self-Adaptive and Self-Organizing Systems*, Venezia, Italy, 2008, pp.129-138.

[4] F. Eady., *Hands-On ZigBee: Implementing 802.15.4 with Microcontrollers*, Oxford: Newnes, 2010.

[5] J. Elson, L. Girod, D. Estrin., Fine-Grained Network Time Synchronization Using Reference Broadcasts, in *Symposium on Operating Systems Design and Implementation*, 2002, pp.147-163.

[6] S. Farahani., *ZigBee Wireless Networks and Transceivers*, Oxford: Newnes, 2011.

[7] R. Gentz, A. Scaglione, L. Ferrari, and Y. Hong., PulseSS: A Pulse-Coupled Synchronization and Scheduling Protocol for Clustered Wireless Sensor Networks, *IEEE Internet of Things Journal*, vol. 3, issue 6, pp. 1222-1234, Dec 2016.

[8] G. Giorgi and C. Narduzzi., Performance Analysis of Kalman-Filter-Based Clock Synchronization in IEEE 1588 Networks, *IEEE Transactions on Instrumentation and Measurement*, vol. 60, issue 8, pp. 2902-2909, Aug 2011.

[9] B. R. Hamilton, X. Ma, Q. Zhao, J. Xu., ACES: Adaptive Clock Estimation and Synchronization Using Kalman Filtering, in *ACM International Conference on Mobile Computing and Networking*, San Francisco, USA, 2008, pp 152-162.

[10] Y. Huang, T. Li, X. Dai, H. Wang, Y. Yang., TS2: A Realistic IEEE1588 Time-Synchronization Simulator for Mobile Wireless Sensor Networks, *SIMULATION*, vol. 91, issue 2, pp. 164-180, Jan 2015.

[11] IEEE Standard for a Precision Clock Synchronization Protocol for Networked Measurement and Control Systems, *IEEE Standard 1588-2008*, 2008.

[12] IEEE Standard for Low-Rate Wireless Networks, *IEEE Standard 802.15.4-2015*, 2015.

[13] T. Jensen and B. Toft. *Graph Coloring Problems*, Wiley, 1995.

[14] R. E. Mirollo and S. H. Strogatz., Synchronization of Pulse-Coupled Biological Oscillators, *SIAM Journal on Applied Mathematics*, vol. 50, issue 6, pp. 1645-1662, 1990.

[15] OMNeT++ release 4.6 (<https://www.omnetpp.org>).

[16] R. Pagliari, Y. Hong, A. Scaglione., Bio-inspired Algorithms for Decentralized Round-Robin And Proportional Fair Scheduling, *IEEE Journal on Selected Areas in Communications*, vol. 28, issue 4, pp. 564-575, Apr 2010.

[17] Atmel SAM R21 Xplained Pro Evaluation Kit.

[18] Y. Zong, X. Dai, Z. Gao, R. Binns, K. Busawon., "Simulation and Evaluation of Pulse-Coupled Oscillators in Wireless Sensor Networks," *Systems Science and Control Engineering*, vol. 6, issue 1, pp. 337-349, Jul 2018.

[19] Y. Zong, X. Dai, Z. Gao, K. Busawon., "Modelling and Synchronization of Pulse-Coupled Non-identical Oscillators for Wireless Sensor Networks," in *International Conference of Industrial Informatics (INDIN)*, Porto, Portugal, 2018 (to be published).